months). In the pseudophakic eyes, the interval ranged from two weeks to 76 months (mean, 11 months; median, eight months). Seven of the patients in our study had had an ultrasonographic examination before enucleation to confirm the diagnosis of malignant melanoma; 17 patients had not undergone such an examination; in 12 patients this information was not given in the clinical history.

Pathologic examination disclosed that the largest dimension of the tumor was less than 10 mm in seven cases, between 10 mm and 15 mm in 11 cases, and larger than 15 mm in 18 cases. The height of the tumor was under 3 mm in one case, between 3 and 5 mm in seven cases, and greater than 5 mm in 28 cases. In eight cases (22.2%) the tumors were of the spindle-cell type, two (5.6%) were of the epithelioid-cell type, 24 (66.6%) were of the mixed-cell type, and two (5.6%) were too necrotic to classify.

Follow-up information on the patients in our study showed that 12 were alive (three with metastatic melanoma) and that ten had died (three with confirmed metastatic melanoma). We were unable to obtain follow-up data in 14 cases.

Discussion

Existing data suggest that uveal malignant melanoma is typically a slow-growing neoplasm that takes several years to reach a significant size.[2,3] Because 80.5% of the tumors in our study (29 of 36 tumors) were more than 10 mm in diameter and the interval between cataract extraction and the diagnosis of the melanoma was usually short (less than one year in 19 of 36, or 52.7%, cases), we believe that most of these tumors were large enough at the time of cataract surgery to have been detected if diagnostic ultrasonography had been performed. In ten cases the unsuspected tumor was probably the cause of a unilateral cataract. This should have heightened the surgeon's suspicion that he was not dealing with a typical senile cataract. We concluded that B-scan ultrasonography should be used in all unilateral cases before extracting a lens if the cataract is too opaque for the fundus to be viewed.

Our experience was similar to that of Shields and Augsburger.[1] They found that 3.3% of 638 patients with uveal melanoma referred to them at the Wills Eye Hospital had had cataract surgery. In none of their 21 cases had the eye been evaluated preoperatively by diagnostic ultrasonography. Of these 21 patients nine had received intraocular lenses. Shields and Augsburger also concluded that preoperative evaluation of a patient with a cataract, particularly if it is unilateral, should include diagnostic ultrasonography. The preoperative examination should also include external examination for ocular melanosis and dilated scleral vessels, slit-lamp examination with the patient's pupil widely dilated for a ciliary body tumor, and transillumination of the eye.

References

1. Shields, J. A., and Augsburger, J. J.: Cataract surgery and intraocular lenses in patients with unsuspected malignant melanoma of the ciliary body and choroid. Ophthalmology 92:823, 1985.

2. Gass, J. D. M.: Observation of suspected choroidal and ciliary body melanomas for evidence of growth prior to enucleation. Ophthalmology 87:523, 1980.

3. McLean, I. W., Foster, W. D., and Zimmerman, L. E.: Uveal melanoma. Location, size, cell type, and enucleation as risk factors in metastasis. Hum. Pathol. 13:123, 1982.

Computerized Quantitative Analysis of Kinetic Visual Fields

Richard G. Weleber, M.D., and Waldo R. Tobler, Ph.D.

Kinetic perimetry is still a widely accepted and used means of assessing the visual field. Attempts at quantifying the area of vision for given isopters have been limited to area measurements on visual field charts, which are azimuthal equidistant polar map projections of the inside surface of the perimetry bowl. Such measurements distort the true size of scotomas (or seeing areas) when the boundaries measured are farther from the center of the field on the chart because of cartographic distortion inherent with this projection. We believe that the solid angle in steradians subtended by the scotoma or the seeing area is a more appropriate measure of the visual field than area on a flat representation. We used a simple computer program to determine the solid angle for given isopters of graphed perimetric visual field data.

DESPITE RECENT INTEREST in automated threshold static perimetry, kinetic perimetry continues to be a widely used technique for assessing the visual field. The most commonly used graph of the kinetic visual field is a flat surface representation of the visual field as mapped on the curved hemispheric surface of the perimetry bowl. Distances, directions, and area cannot be represented perfectly without distortion for any two-dimensional projection of a curved surface. This has led cartographers to produce different map projections of the globe to represent surface area, directions, or distances from a given perspective more correctly. The graphed visual field for kinetic perimetry is an azimuthal equidistant map projection of the inner surface of the perimetry bowl. This means that distances and directions from the center of the graph are correctly represented but area, circumferential distances, and directional relationship other than from the center are not correctly represented. Previous investigators have recognized the distortions inherent in such a projection.[1-5] However, in attempting to quantify the seeing or nonseeing portions of the visual field most investigators measure with a planimeter the seeing area, usually expressed as centimeters squared or degrees squared, encompassed by a given isopter, subtracting the area of scotomas.[6-9] Such measurements distort the true extent of seeing or nonseeing regions farther from the center of the graph. Scotomas in the peripheral visual field occupy a larger surface area on the perimetric chart projection than scotomas of equal size in the central visual field. Mathematical transformation of area measurements obtained from the polar projection can correct for some of the cartographic distortion while introducing others.[4]

A set of lines radiating from a given point, such as a cone from its apex, are said to subtend a solid angle (Fig. 1). A better way of expressing the magnitude of the visual field for a given isopter is the solid angle subtended by the seeing region of the visual field minus the solid angle of any scotomas with the same test target within that isopter. The most common unitary measure of a solid angle is the steradian, which is the three-dimensional counterpart to the two-dimensional degree. Imagine lines emanating from the center of a sphere of radius, r, which cut the surface of the sphere to

Accepted for publication Jan. 20, 1986.

From the Departments of Ophthalmology and Medical Genetics, Oregon Health Sciences University, Portland, Oregon (Dr. Weleber); and the Department of Geography, University of California, Santa Barbara, California (Dr. Tobler). This study was supported in part by the National Retinitis Pigmentosa Foundation, Fighting Blindness, Baltimore, Maryland, and BRSG S07 RR05412 Award by the Biomedical Research Support Grant Program, Division of Research Resources, National Institutes of Health.

Reprint requests to Richard G. Weleber, M.D., Oregon Health Sciences University, 3181 S.W. Sam Jackson Park Rd., Portland, OR 97201.

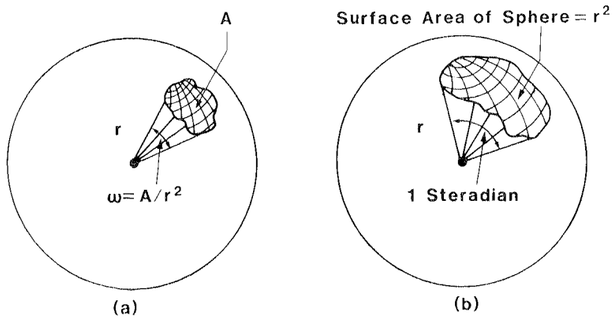

Fig. 1 (Weleber and Tobler). The solid angle, ω, is defined as the surface area, A, cut by lines emanating from the center of a sphere of radius r, divided by the radius squared (left). The steradian is that solid angle where the surface area on the sphere equals the radius squared (right).

create an area, A. A solid angle of one steradian cuts the surface of the sphere to form an area equal to r^2 (Fig. 1). Since the total surface area of a sphere is $4\pi r^2$, the total solid angle of a sphere is 4π steradians. A hemisphere subtends 2π (or approximately 6.283) steradians. The normal visual field for large, bright test objects subtends about 4.1 steradians. The normal blind spot subtends only approximately 0.012 steradian.

The best method for determining the solid angle of the kinetic perimetric visual field is to transfer the sampling points for an isopter of a given test size and brightness onto the surface of a sphere and to determine the area of the polygon so created. The solid angle, in steradians, is then proportional to this area. We present a simple computer program that converts polar coordinates, distance RD and direction TD, as measured from perimetric charts, to points on the surface of a sphere, and then computes the area of the polygon and the solid angle subtended by this area.

Methods

An abbreviated version of the program that illustrates the algorithms involved was written in GWBasic, Version 2.02 R2.1, using double precision, on an AT&T PC 6300 (Fig. 2). This program will run as listed without modification in BASICAID on the IBM PC and in Microsoft Basic for the Macintosh, Version 2.00.00, Binary Math, on the Apple computer. The program inputs polar distances in degrees, RD, in lines 190–220 and directions, TD, in lines 230–260, for one quadrant of a hemisphere, or one-eighth of the surface of a sphere, or ½π (1.571) steradians. In lines 360–420 the distances and directions are converted from degrees to radians, R and T. Note that distances at 90 degrees are constrained to less than 90 degrees. The program as written computes the solid angle only out to 90 degrees from center. Distances greater than 90 degrees project onto the other hemisphere, but can be measured separately by determining the solid angle subtended by points reflected equidistant from 90 degrees toward the center of the graph. This value is then added to the solid angle determined with that isopter within 90 degrees. Lines 430–600 project the coordinates onto the surface of a sphere and compute the solid angle, in steradians, subtended by the polygon which has been created. The percent of the surface of a sphere is computed at line 620.

Figure 3 lists program lines that, when typed into the program shown in Fig. 2, allow entry of data from the keyboard. (Lines 165, 250, and 260 must be deleted.)

We have written a longer, more complex program that processes multiple-array storage files of digitized visual field data created by the x,y coordinate function within the Digitizing Morphometry program of the Bioquant II Image Analysis System (Version Jan. 9, 1985). This system utilizes a Hipad digitizing tablet with a resolution of 0.1 mm. Our larger program reads into memory the digitized visual field x,y coordinates stored on flexible disks, converts the x,y coordinates to cartesian coordinates, converts the cartesian coordinates to polar distances and directions, both in radians, R and T, and in degrees, RD and TD, and then proceeds to compute the solid angle in steradians and the percent of the surface of a sphere for all isopter data previously digitized. The output of this program for a normal visual field, shown in Figure 4, is listed in Table 1. Note that if one for the moment disregards the


```
100 REM SOLID ANGLE OF SPHERICAL POLYGON
110 REM FROM DISTANCES, RD, AND DIRECTIONS, TD (IN DEGREES)
120 REM R. WELEBER AND W. TOBLER 14 NOV 85
130 REM PROGRAMMED ON AT&T PC 6300 IN GWBASIC/D (DOUBLE PRECISION)
140 REM FOR IBM PC USE BASICA/D
150 DEFDBL A,D,E,P,R,T,X,Y
160 PI=3.1415926535897793#
165 N=11:GOTO 180:REM CURRENT DATA HAS 11 PAIRS
170 INPUT "NUMBER OF DATA PAIRS";N
180 DIM RD(N),TD(N),R(N),T(N)
190 FOR I=1 TO N
200    READ RD(I)
210 NEXT I
220 DATA 0,90,90,90,90,90,90,90,90,90,90
230 FOR I=1 TO N
240    READ TD(I)
250 NEXT I
260 DATA 0,180,190,200,210,220,230,240,250,260,270
270 R1=180/PI
280 PRINT:PRINT:PRINT:PRINT N;" OBSERVATIONS"
290 PRINT "POLAR DISTANCES, DIRECTIONS"
300 PRINT "(in degrees)"
310 FOR I=1 TO N
320    IF I<10 THEN PRINT " ";
330    PRINT I;RD(I);TD(I)
340 NEXT I
350 PRINT
360 REM CONVERT TO RADIANS
370 FOR I=1 TO N
380    IF RD(I)<90 THEN 400
390    RD(I)=90#
400    R(I)=RD(I)/R1
410    T(I)=TD(I)/R1
420 NEXT I
430 REM SET RADIANS
440 A=0
450 FOR I=1 TO N
460    K=I+1
470    IF K<=N THEN 490
480    K=1
490    D1=ABS(T(I)-T(K))*.5
500    IF D1=0 THEN 600
510    X=(R(K)-R(I))*.5
520    Y=(R(K)+R(I))*.5
530    T1=1/TAN(D1)
540    D3=COS(X)/COS(Y)*T1
550    D3=2*ATN(D3)
560    E=D3+2*D1-PI
570    IF T(K)=>T(I)  THEN  590
580    E=-E
590    A=A+E
600 NEXT I
610 PRINT "Solid Angle = ";A;" steradians"
620 PAS=A/(4*PI)*100
630 PRINT "  or ";PAS;" % of Sphere"
640 FOR K=1 TO 5:PRINT:NEXT K:END
```

Fig.

```
190 PRINT "PAIR","DISTANCE (RD), DIRECTION (TD)"
200 PRINT ,"AS RD,TD"
210 FOR I=1 TO N
220     IF I<10 THEN PRINT " ";
230     PRINT I;:INPUT "                ";RD(I),TD(I)
240 NEXT I
```

Fig. 3 (Weleber and Tobler). Program lines that alter program listed in Figure 2 so that distances, RD, and directions, TD, can be entered from the keyboard. Lines 165, 250, and 260 in Figure 2 must be deleted.

solid angle subtended by the blind spot, the normal visual field within 90 degrees with the IV_4e test target subtends 4.058 steradians or 32.3% of the surface of a sphere. The rim of visual field beyond 90 degrees subtends 0.056 steradian or 0.44% of the surface of a sphere. To obtain the net solid angle of seeing area with any given isopter, one must subtract the solid angles subtended by scotomas within the seeing area. If one assumes that the blind spot for the IV_4e test target is essentially the same as for the I_4e test target (0.012 steradian), the total solid angle for the IV_4e test target is 4.102 steradians (4.058 + 0.056 −0.012) or 32.6% of the surface of a sphere. Without subtracting the solid angle of the blind spot, the I_2e isopter subtends 1.565 steradians, approximately one-eighth of the surface of a sphere.

Figure 5 is the visual field of a patient who has retinitis pigmentosa with midperipheral scotomas and contracture of isopters. Table 2 is the computer output for these data. Note that the I_4e isopter for the patient with retinitis pigmentosa subtends only 0.110 steradian compared to 3.377 −0.012 or 3.365 steradians for the normal visual field. Stated differently, the solid angle for the I_4e isopter for the patient with retinitis pigmentosa is only 3.3% of normal. The IV_4e isopter solid angle was 2.144 −(0.019 + 0.375) = 1.750 steradians, or about 43% of normal.

Figure 6 depicts the positioning of a 3-cm² hexagon, representing a theoretic scotoma, centered at varying degrees of eccentricity on a standard kinetic perimetry chart. Table 3 is the computer output for the solid angles and the percents of surface of a sphere for these identical figures. Note that the solid angle of this polygon projected upon the surface of a sphere decreases as the figure is centered eccentrically. In the far periphery, the cartographic distortion reduces the solid angle of the hexagon by

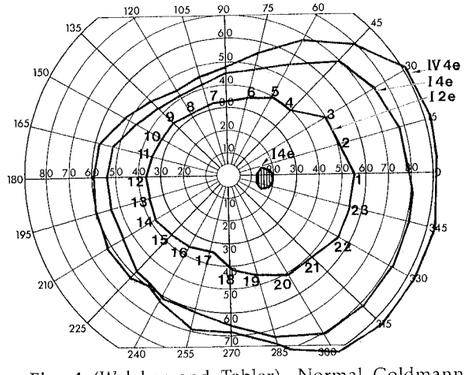

Fig. 4 (Weleber and Tobler). Normal Goldmann kinetic visual field. Numbers along I_2e isopter are sampling points where target was first seen. The polar distances and directions representing these points are shown in Table 1.

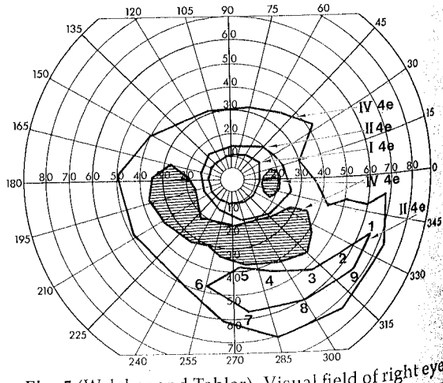

Fig. 5 (Weleber and Tobler). Visual field of right eye of a 41-year-old man with type 2 Usher's syndrome (retinitis pigmentosa and partial congenital deafness). Note numbers along isopter sampling points for the peripheral seeing area with the II_4e test target. The polar distances and directions for these points are shown in Table 2.

TABLE 1
OUTPUT OF PROGRAM FOR NORMAL VISUAL FIELD

	PERIMETRIC FIELD MEASUREMENT DATA*							
ISOPTER	1 (I_2e)		2 (I_4e)		3 ($-I_4e$)		4 (IV_4e)	
POINTS	RD	TD	RD	TD	RD	TD	RD	TD
1	54.7	1.0	77.6	14.9	18.2	4.2	90.0	4.2
2	51.0	14.9	74.9	30.5	17.4	9.1	90.0	15.4
3	50.2	29.7	69.1	45.5	16.1	11.3	90.0	30.2
4	40.2	45.7	55.6	60.4	14.9	12.3	79.1	45.2
5	39.4	59.6	48.0	75.0	13.2	9.0	67.2	60.4
6	35.6	73.6	45.5	90.3	12.2	0.4	54.8	75.5
7	32.7	100.4	42.1	104.6	12.7	348.3	47.4	90.4
8	31.9	118.7	41.5	119.4	14.1	342.5	45.4	104.6
9	33.6	135.1	42.9	134.7	16.0	341.5	44.0	120.0
10	33.4	149.5	46.4	149.5	17.6	343.8	47.3	135.3
11	34.6	164.8	52.2	165.0	18.4	348.2	51.8	149.6
12	36.5	179.6	53.5	179.7	18.6	354.1	57.8	165.2
13	35.7	195.3	53.2	195.3	0.0	0.0	58.7	180.0
14	37.3	210.7	54.3	210.2	0.0	0.0	60.0	195.3
15	36.2	225.3	58.6	225.1	0.0	0.0	61.6	210.2
16	35.6	241.0	58.8	235.0	0.0	0.0	62.1	225.2
17	34.3	258.1	61.2	240.3	0.0	0.0	59.3	233.3
18	41.4	270.7	61.8	255.3	0.0	0.0	62.9	240.3
19	45.3	285.0	65.7	270.3	0.0	0.0	69.2	255.0
20	50.6	299.9	73.8	285.2	0.0	0.0	68.4	270.0
21	51.0	314.8	80.5	299.7	0.0	0.0	77.2	285.2
22	54.8	329.9	81.5	314.8	0.0	0.0	80.8	288.4
23	54.4	344.6	81.3	330.1	0.0	0.0	90.0	299.7
24	0.0	0.0	80.7	345.0	0.0	0.0	90.0	315.4
25	0.0	0.0	80.3	353.9	0.0	0.0	90.0	328.9
26	0.0	0.0	0.0	0.0	0.0	0.0	90.0	344.6

ISOPTER NO.	TEST TARGET	SOLID ANGLE SUBTENDED	% OF SPHERE
1	I_2e	1.565	12.46
2	I_4e	3.377	26.87
3	$-I_4e$	0.012	0.10
4	IV_4e	4.058	32.29

* Digitized distances (RD) and directions (TD), solid angles (in steradians), and percents of surface of sphere for isopter data within 90 degrees from visual field in Figure 4. Minus signs indicate a scotoma (the blind spot) with this test target. Compare distances and directions for the I_2e isopter points with the positions on the perimetric chart in Figure 4.

31%. Conversely, a given nonseeing region in the far peripheral visual field would occupy up to 45% more surface area than a central scotoma of equal size when both are plotted on the standard perimetric chart. In other words, conventional planar representation of the kinetic visual field overestimates the size of scotomas in the far peripheral visual field by as much as 45%.

Discussion

Although inspection of visual fields usually gives the clinician all the information needed, quantification of the visual field is necessary when statistical analysis of rate of change with time or significance of change is desirable. Previous attempts at reducing visual field data

TABLE 2
OUTPUT OF PROGRAM OF PATIENT WITH RETINITIS PIGMENTOSA WITH MIDPERIPHERAL SCOTOMAS AND CONTRACTURE OF ISOPTERS

	PERIMETRIC FIELD MEASUREMENT DATA*											
ISOPTER	1 (I_4e)		2 (II_4e)		3 (II_4e)		4 (IV_4e)		5 ($-IV_4e$)		6 ($-IV_4e$)	
POINTS	RD	TD	RD	TD	RD	TD	RD	TD	RD	TD	RD	TD
1	13.5	30.1	23.4	13.0	65.5	336.7	29.5	13.9	19.9	5.5	34.9	335.7
2	11.9	55.9	19.9	31.3	58.3	324.9	42.4	33.0	18.0	12.3	27.6	331.3
3	10.4	74.6	18.2	46.7	52.4	310.2	34.9	53.5	17.1	13.0	23.5	316.9
4	10.3	107.4	14.4	90.3	43.4	292.3	31.4	74.3	14.0	6.8	20.5	274.0
5	10.2	149.0	14.7	131.6	38.6	273.5	30.7	107.9	12.6	352.8	21.7	230.8
6	10.3	178.1	13.8	166.0	47.8	257.0	40.2	152.2	14.2	339.4	16.2	199.3
7	10.5	210.7	13.5	197.2	57.6	276.2	49.9	179.0	17.6	334.2	18.3	180.3
8	10.6	243.8	14.3	245.2	60.9	299.7	49.8	208.0	19.4	341.2	25.7	165.6
9	10.6	269.1	18.4	282.8	65.6	322.1	50.8	245.2	20.8	351.3	34.1	179.0
10	11.3	301.5	22.5	316.4	0.0	0.0	61.2	264.4	0.0	0.0	36.5	194.4
11	11.5	330.1	26.1	347.6	0.0	0.0	71.0	285.3	0.0	0.0	34.7	211.4
12	11.6	358.8	0.0	0.0	0.0	0.0	73.9	309.8	0.0	0.0	32.0	228.4
13	0.0	0.0	0.0	0.0	0.0	0.0	73.1	335.0	0.0	0.0	32.1	235.3
14	0.0	0.0	0.0	0.0	0.0	0.0	67.8	352.1	0.0	0.0	30.1	249.3
15	0.0	0.0	0.0	0.0	0.0	0.0	60.0	347.5	0.0	0.0	33.9	259.2
16	0.0	0.0	0.0	0.0	0.0	0.0	50.5	348.5	0.0	0.0	37.0	277.8
17	0.0	0.0	0.0	0.0	0.0	0.0	43.4	343.3	0.0	0.0	41.6	300.0
18	0.0	0.0	0.0	0.0	0.0	0.0	36.3	356.6	0.0	0.0	45.9	315.1
19	0.0	0.0	0.0	0.0	0.0	0.0	0.0	0.0	0.0	0.0	41.2	325.4

ISOPTER NO.	TEST TARGET	SOLID ANGLE SUBTENDED	% OF SPHERE
1	I_4e	0.110	0.88
2	II_4e	0.284	2.26
3	II_4e	0.215	1.71
4	IV_4e	2.144	17.06
5	$-IV_4e$	0.019	0.15
6	$-IV_4e$	0.375	2.98

* Digitized distances (RD) and directions (TD), solid angles (in steradians), and percents of sphere for isopter data in Figure 5. Minus signs indicate scotoma (blind spot is isopter 5). Compare sampling points on the visual field chart in Figure 5 with the polar distances and directions for the sampling points for the peripheral II_4e seeing area (RD and TD in columns for isopter 3).

to numeric variables have concentrated on chart area measurements with planimeters, which not only do not correct cartographic distortions but which may also introduce additional inaccuracies. Techniques in which straight lines are digitized between points on the perimetry chart actually create data points that do not exist on the surface of a sphere. A straight line on the polar projection perimetry chart is not the shortest surface distance between two points on the surface of a sphere. This can be readily appreciated, for example, by connecting every other data point. Thus, our method of determination of the solid angle is also preferable because it avoids the creation of extraneous data points.

The major source of error in determining the true solid angle subtended by a given test target with our method remains, as it does with kinetic visual fields in general, with the sampling error inherent in measuring a finite number of points. Measuring seeing or nonseeing regions of the visual field with more data points will define the polygon on the surface of the sphere with greater precision.

Our method gives the best estimation of the visual field as mapped on the inner surface of the perimeter. The solid angle of seeing or

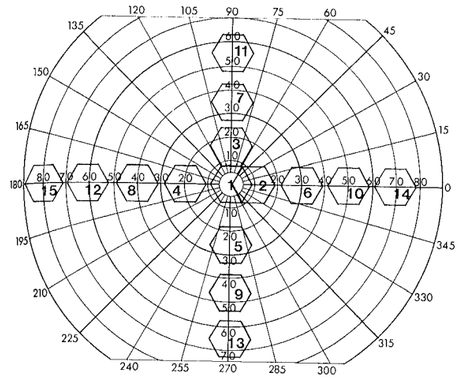

Fig. 6 (Weleber and Tobler). Positioning of 3-cm² hexagons on standard perimetric chart. Table 3 shows the computer output for these hexagons.

scotomatous regions of the visual field should become a useful criterion for evaluation of the visual field in all patients with visual field defects. There still exist distortions in the representation of the visual field with regard to retinal eccentricity.[10-13] Thus, the solid angle of visual field defects produced by lesions of equal size in the peripheral retina and central retina will not correspond exactly. Mathematical correction for distortion of retinal eccentricity could be incorporated into our model, but this involves certain approximations and assumptions, in that the shape of the posterior segment of the normal eye is not only complex but varies among individuals. For example, there is considerable difference in the shape of a myopic eye.

Legal blindness from constriction of visual field is presently defined as 20 degrees or less of remaining central field in the better eye as measured with the III_4e test target on a Goldmann perimeter.[14] Whereas this is an appropriate determination for the patient with concentric visual field loss, pericentral ring scotomas that encroach upon fixation may be associated with sufficient visual acuity to exclude legal blindness on the basis of loss of central visual acuity but still produce severe visual disability. One could adjust the visual field representation to weigh to a greater degree the central regions where photoreceptor density is highest[1] or neural acuity is greatest.[11] Visual field projections that reflect specific photoreceptor density would be useful for assessing the extent of

TABLE 3
OUTPUT PROGRAM FOR A THEORETIC SCOTOMA*

HEXAGON NO.	LOCATION	SOLID ANGLE SUBTENDED	% OF SPHERE
1	CENTER	0.0617	0.491
2	10 DG	0.0606	0.482
3	15 DG	0.0620	0.494
4	20 DG	0.0609	0.485
5	25 DG	0.0593	0.472
6	30 DG	0.0589	0.469
7	35 DG	0.0589	0.468
8	40 DG	0.0561	0.447
9	45 DG	0.0572	0.455
10	50 DG	0.0537	0.428
11	55 DG	0.0522	0.415
12	60 DG	0.0513	0.409
13	65 DG	0.0494	0.393
14	70 DG	0.0472	0.376
15	80 DG	0.0424	0.337

* Solid angles (in steradians) and percents of the surface of a sphere for the hexagons in Figure 6 at various degrees of eccentricity.

involvement in disorders such as retinitis pigmentosa. Projections that better represent neural retinal acuity, by emphasizing the importance of central regions of the visual field, would be more appropriate than the standard perimetric charts for determination of disability. We are currently working on a computer program that will plot digitized standard perimetric data as projections better representing retinal area, photoreceptor density, or neural acuity. The program that we have described provides a first step in such improved visual field quantification.

References

1. Doesschate, J. T.: Perimetric charts in aequivalent projection allowing a planimetric determination of the extension of the visual field. Ophthalmologica 113:17, 1947.
2. Dannheim, F.: Non-linear projection in visual field charting. Doc. Ophthalmol. Proc. Ser. 35:217, 1983.
3. Frísen, L.: The cartographic deformations of the visual field. Ophthalmologica 161:38, 1970.
4. Kirkham, T. H., and Meyer, E.: Visual field area